

## POROUS TITANIUM - AN ENHANCED SUPPORT FOR HUMAN OSTEOBLASTS AFTER ANODIZATION AND c-RGD IMMOBILIZATION

ANA-MARIA SALANTIU<sup>a,\*</sup>, OLGA SORITAU<sup>b</sup>, NOEMI DIRZU<sup>b</sup>,  
FLORIN POPA<sup>a</sup>, LIANA MURESAN<sup>c</sup>, VIOLETA POPESCU<sup>a</sup>,  
PETRU PASCUTA<sup>a</sup>, CATALIN POPA<sup>a</sup>

**ABSTRACT.** Porous titanium is the material of choice for hard tissue implants but an enhanced osseointegration can be achieved only through subsequent surface conditioning. In this work, we aimed to study the effect of both surface conditioning and immobilization of cyclic Arg-Gly-Asp (RGD) peptide onto two types of porous titanium samples designed for endosseous applications and obtained by Powder Metallurgy (PM) in view of osteoblast cells attachment and proliferation. Cyclic RGD peptide was chosen as bioactive target and was covalently immobilized on anodized PM porous titanium. The samples, formerly pressed with 200 or 400 MPa and sintered at 1100°C in vacuum, were first anodized using a constant voltage of 2V for 1 hour with 0.25 M sulphuric acid to enhance the thickness of titanium oxide layer. An intermediary aminoalkylsilane molecule (APTES) was then covalently linked to the oxide layer, followed by the covalent binding of cyclic RGD peptide to the free terminal NH<sub>2</sub> groups using polyethyleneglycol diglycidyl ether (PEGDE) as coupling agent. The samples were characterized by micro CT, X-ray diffraction (XRD), scanning electron microscopy (SEM) and Fourier transform infrared spectroscopy (FT-IR). Anodized titanium samples display anatase and rutile on the surface and, after functionalization, two important amide characteristic regions, confirming the presence of cyclic RGD peptide. Cells seeded on samples pressed with 400 MPa, anodized and c-RGD immobilized, displayed a more flattened shape and a more obvious tendency of spreading into pores.

**Keywords:** porous titanium, cyclic RGD, anodic oxidation, human osteoblasts

---

<sup>a</sup> Technical University of Cluj-Napoca, Faculty of Materials and Environmental Engineering, 103-105 Muncii Avenue, RO-400641, Cluj-Napoca, Romania,

<sup>b</sup> "Prof. I.Chiricuta" Oncological Institute, 34-36 Republic str., RO- 400015, Cluj-Napoca, Romania,

<sup>c</sup> Babeş-Bolyai University, Faculty of Chemistry and Chemical Engineering, 11 Arany Janos str., RO-400028, Cluj-Napoca, Romania.

\* Corresponding author: bolfa\_anamaria@yahoo.com

## INTRODUCTION

Ti and Ti alloys are intensively studied for most dental and orthopedic applications [1,2]. Porous structures gained an increased interest for medical applications due to their low elastic modulus, matching that of bones [3,4]. A porous surface enhances the implant/ bone bonding by growth of tissue into the pores [5]. To this aim, it was reported that the optimal pore size for bone ingrowth should be between 100  $\mu\text{m}$  and 600  $\mu\text{m}$  [6]. Besides the use of porous surfaces, osseointegration of titanium implants is influenced also by surface properties which are often the basis of successful endosseous implantology [7,8]. Various techniques have been studied and applied to improve the osseointegration of titanium implants [9], such as acid etching, plasma spraying, anodizing [10,11] and also by the use of bioactive coatings [12]. Titanium surface conditioning *via* anodizing has been reported to increase the surface area and the activity of the contacting cells [13]. On the other hand, bioactive coatings have the role to create a strong interface between bone tissues and implant [14]. It is fundamental that the method used to attach a biomolecule to the implant surface is stable enough to keep the biomolecule in place until the desired response is triggered [15].

A method commonly employed to covalently attach biomolecules onto hydroxylated surfaces is functionalization using an aminosilane reaction and subsequent chemical attachment using crosslinkers [15,16]. 3-Aminopropyltriethoxysilane (APTES) is a silane molecule commonly used in the biomedical literature to bond an assortment of materials [16]. The presence of  $\text{NH}_2$  end groups on the silanized surface has a major importance in biological applications as it allows proteins or other biomolecules to be attached in a simple way [17]. Bioactive peptides have been used to promote cell adhesion, in particular extensive scientific investigations have been described using RGD peptide, a short amino acid sequence present in several adhesive extracellular matrix proteins, for improving cell adhesion *via* cell membrane integrins reactions [18-20]. It was reported that RGD-related peptides influence also osteoblast mineralization, cytoskeleton reorganization and migration *in vitro* [21].

The purpose of this study was to evaluate the influence of both surface conditioning and c-RGD peptide immobilization on porous titanium with respect to osteoblast adhesion and proliferation.

## RESULTS AND DISCUSSION

### Microstructural analysis of porous titanium samples

The linear analysis performed on optical images of surfaces revealed an average porosity of 33% for samples pressed with 200 MPa

and 28% for 400 MPa pressed ones, while the average pore size was of 31  $\mu\text{m}$  and 26  $\mu\text{m}$  respectively. Nevertheless, large pores with the conventional diameter of more than 100  $\mu\text{m}$  can be observed for both types of samples (Figure 1a and b). The shape of pores is irregular, with sharp edges; interconnected pores are representing the majority, as it can be observed also by micro CT images of the cross section of samples (Figure 1b'). This aspect of structure is well suited for osseointegration, while providing a low Young's modulus.

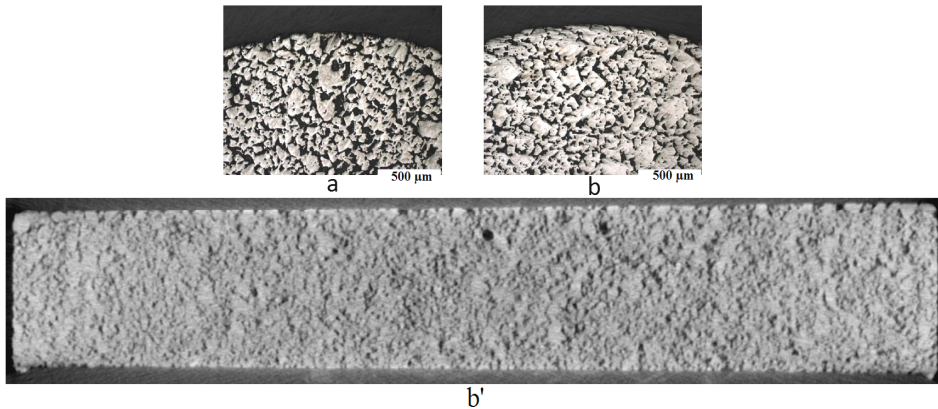


**Figure 1.** Optical images for titanium pressed samples with 200 MPa (a) and 400 MPa (b) and microCT image for the titanium sample pressed with 400 MPa (b').

### **Electrochemical behaviour of anodized PM porous titanium**

To inspect the influence of manufacturing conditions for the titanium samples pressed with 200 or 400 MPa, chronoamperometric tests were devoted to analyse the influences upon the titanium oxide formation. The curves are shown in Figure 2. The current density / time measurements showed that overall process can be described in two stages. The first stage represents the nucleation of a titanium oxide layer on the porous surface, which lowers the current density in the circuit. In the last stage, the current density remained stable, increasing the thickness of the titanium oxide layer.

When comparing the chronoamperograms results for the different types of titanium samples, Figure 2, it was found that samples pressed with 200 MPa presented the highest intensity of oxidation / dissolution reactions. Such behaviour is explained by the increased active surface of the electrode. In contrast, the curve for the sample pressed with 400 MPa, after the first stage, present an increasing tendency of current density, a certain

instability, which could be related with the sharp edges pores that are more pronounced on this sample (see Figure 1).

### **Lattice structure of anodized Ti oxide**

Figure 3 shows the XRD patterns for untreated porous titanium and anodically oxidized porous titanium in 0.25 M H<sub>2</sub>SO<sub>4</sub> for 1 hour at 2V and then heat treated at 700°C. For any temperature of the heat treatment below 700°C, no peak corresponding to any of the oxides occurred. Only the peaks of titanium could be observed for the untreated porous Ti sample (Figure 3a). The peaks of rutile and anatase occurred for titanium samples pressed with 200 MPa and then oxidized at 2V (Figure 3b). From Figure 3c it can be seen that a higher compaction pressure of 400 MPa resulted in a decrease of the peak intensity of the rutile phase while no peaks for anatase phase appeared. The trends in anatase and rutile formation should be attributed to the higher thermodynamic stability of the rutile phase with respect to the anatase phase, which makes rutile more likely to form. The differences in the oxide nucleation and growth for the two types of samples, as seen in Figures 2 and 3, are supposed to be generated by the effects at the bottom of pores, as both porosity and pores size display small differences.

### **Chemical functionalization of anodized porous titanium surfaces and cyclic RGD immobilization**

FTIR spectra in the range from 4000 cm<sup>-1</sup> to 500 cm<sup>-1</sup> for APTES and PEGDE/c-RGD films grafted on the porous titanium surfaces are shown in Figures 4 and 5. APTES films prepared from toluene solution show similar features in the range presented before, on the anodized titanium samples pressed with 200 and 400 MPa (Figures 4b and 5b). Around 3400 cm<sup>-1</sup>, the symmetric and asymmetric –NH stretch modes from amino group in APTES were very weak in the spectra. In Figure 4b and also in Figure 5b, between 2800 and 3000 cm<sup>-1</sup> are found several CH stretch modes corresponding to APTES backbone and ethoxy groups [14]. The most important structural information regarding APTES films is found between 1800-900 cm<sup>-1</sup>. A vibrational mode around 1655 cm<sup>-1</sup> is due to the presence of an imine group formed by the oxidation of an amine bicarbonate salt. Two dominating vibrational modes are found around 1575 and 1485 cm<sup>-1</sup>. Such vibrational modes arise when surface amino groups form bicarbonate salts in a reaction with atmospheric CO<sub>2</sub>, as was reported previously [22]. The mode near 1195 cm<sup>-1</sup> arise from unhydrolyzed ethoxy moieties in APTES (-OCH<sub>2</sub>CH<sub>3</sub>). The peak located around 1110 cm<sup>-1</sup> is attributed to Si-O-Si from polymerized APTES indicating that the silane agent had been grafted onto the surface of anodized titanium surfaces [23].

Curing of silanes at elevated temperature, 110°C, seemed to enhance the siloxane layer formation on the TiO<sub>2</sub> surface of titanium substrate.

FTIR spectra corresponding to PEGDE/c-RGD peptide films grafted on silanized titanium samples pressed with 200 and 400 MPa are presented in Figures 4c and 5c. The intense band at approximately 2870 cm<sup>-1</sup> was attributed to the symmetric stretch of the methylene group. Bands in the region 1500-1100 cm<sup>-1</sup> were generally due to the bending, wagging and twisting modes of the CH<sub>3</sub> and CH<sub>2</sub> groups and the methylenes of the O-CH<sub>2</sub>-CH<sub>2</sub>-O group. The most intense band at 1093 cm<sup>-1</sup> was assigned to the asymmetric C-O-C stretch [24].

The ATR-FTIR spectrum of c-RGD-PEGDE for both of the two types of samples show all the characteristic peaks presented before, which demonstrates that c-RGD/PEGDE films have the similar base structure as PEGDE films. However, cRGD/PEGDE films show two more important characteristic regions at 1650 cm<sup>-1</sup> and at 1559 cm<sup>-1</sup>, which correspond to the vibrations of amide (-CO-NH) I and II, respectively [25].

These amide groups are from the c-RGD peptide, indicating that c-RGD peptide is present on the films surface anchored on porous titanium samples.

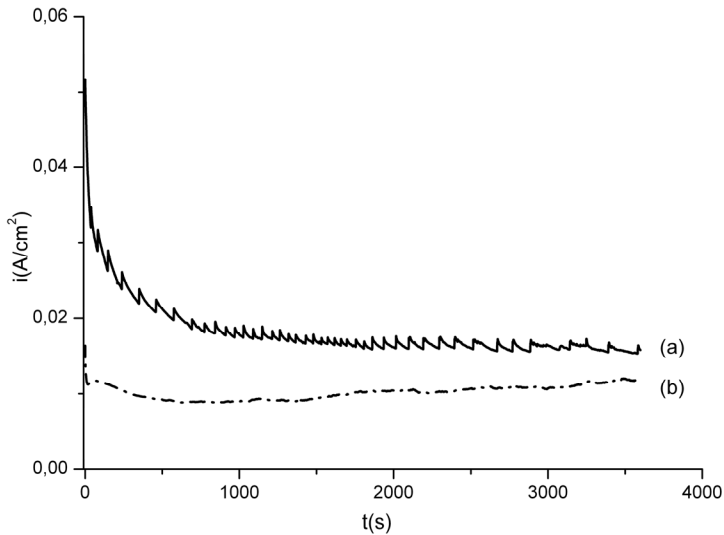


**Figure 2.** Chronoamperograms for anodic oxidation of titanium samples pressed with 200 MPa (a) and 400 MPa (b).

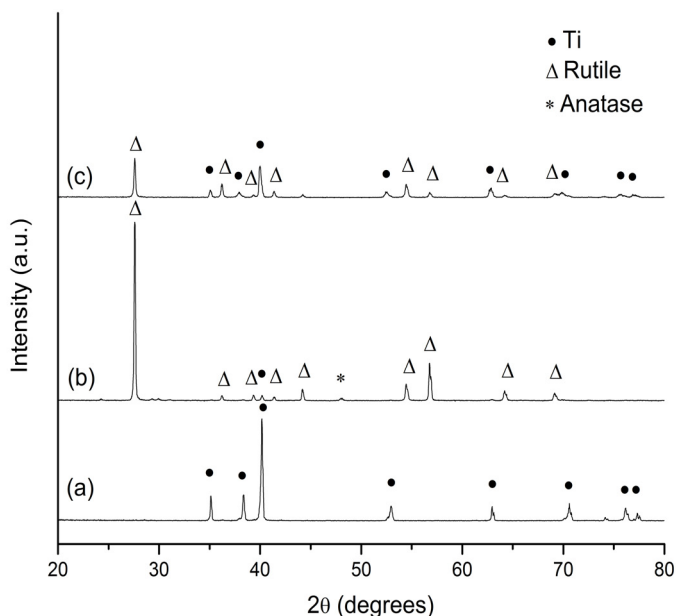


**Figure 3.** XRD patterns of untreated porous titanium (a) and anodized titanium samples pressed with 200 MPa (b) and 400 MPa (c) at 2V for 1h and then heat treated at 700°C.

### Adhesion and proliferation of human osteoblasts

Adhesion and proliferation were evaluated on untreated and on modified ( $\text{TiO}_2$ , c-RGD) porous titanium samples. To assess cell attachment and morphology, PKH26 marked osteoblast cells were analysed by fluorescence microscopy after 1 hour, 4 days and 14 days of cultivation on the samples mentioned before. The presence of c-RGD peptide increased cell attachment one hour after seeding on both 200 and 400 MPa titanium pressed samples (Figure 6a). After 4 days of osteoblasts cultivation, 200 and 400 MPa titanium pressed samples coated with c-RGD peptide (Figure 6b), sustained a higher number of cells. Cell spreading was observed especially on anodized titanium samples. The best cell proliferation rate after 14 days was observed for c-RGD coated samples pressed with both 200 and 400 MPa, Figure 6c, as well as for untreated and anodized titanium samples pressed with 400MPa.

Cells counting of PKH26 stained cells was performed after the capture of images in three different microscopic fields randomly selected and the obtained results are shown in Figure 7 as cells number/mm<sup>2</sup>. After one hour, 400 MPa-RGD samples displayed by far the highest number of attached cells, while the 400 MPa-anodizing samples displayed the lowest. The latter one might be due to the oxidation instability proven in Figure 2b. The same trend could be observed after 4 hours, but all differences were smaller. After 14 days, the highest number of cells corresponds to 400 MPa-anodizing samples and RGD samples come after. The increased fluorescence intensity observed in the optical images for c-RGD coated samples (Figure 6), could be explained by the presence of cells on the RGD samples surface due to cell capture by the peptide sequences, capture which does not allowed their migration into the pores of the samples, as in the case of only anodized samples. For these ones, it seems that along the 14 days, the oxide layer became stable enough.

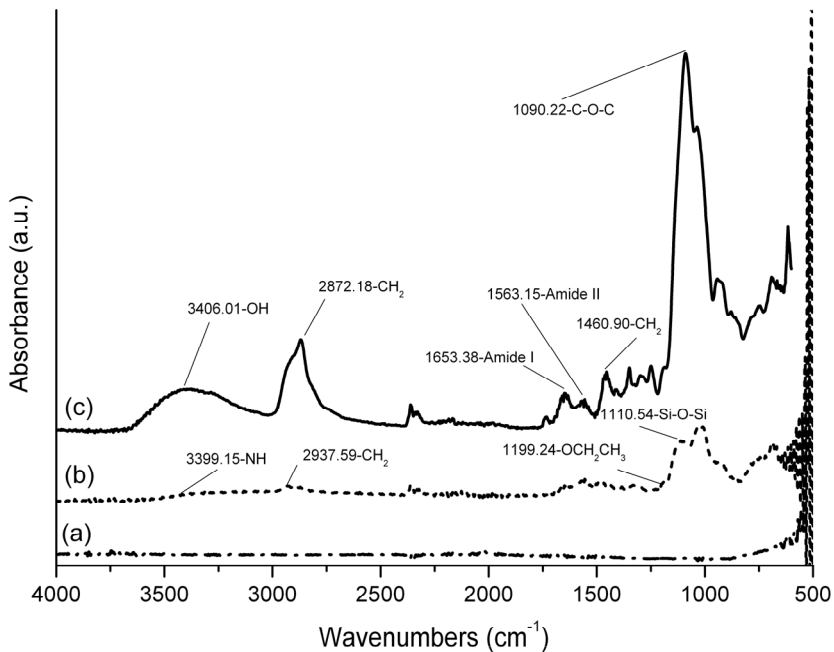


**Figure 4.** FTIR spectra of (a) anodized, (b) silanized and (c) c-RGD peptide grafting on titanium sample pressed with 200 MPa.

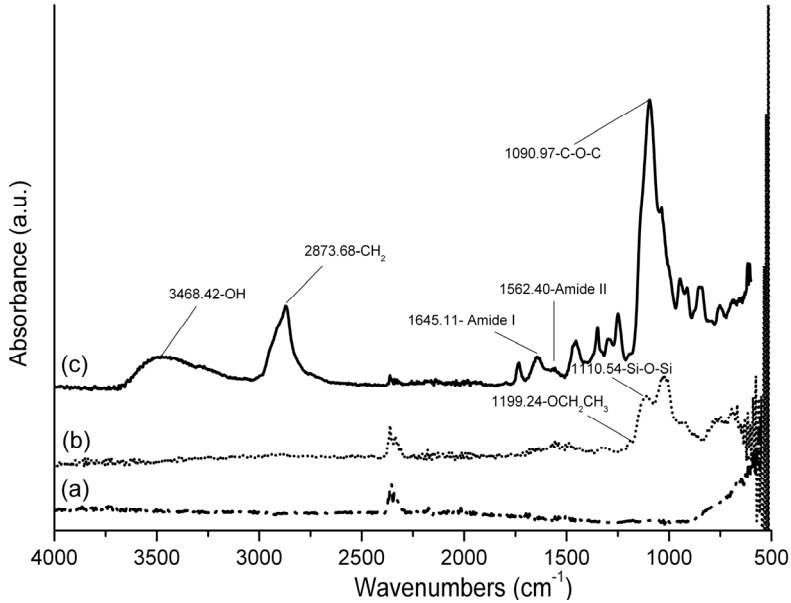


**Figure 5.** FTIR spectra of (a) anodized, (b) silanized and (c) c-RGD peptide grafting on titanium sample pressed with 400 MPa.

### SEM morphological analysis

Figure 8 illustrates the surface SEM micrographs of untreated and modified titanium samples pressed with 200 and 400 MPa without and with osteoblast cells. After 29 days of culture, cells on untreated titanium samples pressed with 400 MPa, Figure 8a, appeared in higher number, more spread and with traces of mineralization in comparison with the sample pressed with 200 MPa. On the anodized titanium sample pressed with 200 MPa without osteoblast cells seeded, Figure 8b, an advanced coverage of the pores with a titanium dioxide layer occurred. For the other type of samples, the difference between untreated and anodized state is not so visible because the coverage with a titanium dioxide layer was reduced. In Figure 8b it can be seen that the osteoblast cells migrated and adhered into the pores of anodized titanium samples, which is consistent to the conclusions for Figure 7.

The presence of c-RGD peptide attachment on the surface of TiO<sub>2</sub> after coating with an intermediate layer of APTES without osteoblast cells seeded was observed as irregular deposits. For the titanium sample pressed with 400 MPa and coated with c-RGD, (Figure 8c), we can observe

the presence of c-RGD attachment at the surface but also in the pores. The presence of the c-RGD peptide on titanium samples pressed with 400 MPa induced a more flattened cell shape with tendency of cell spreading into pores in contrast with the round shape of cells cultivated on c-RGD surface coated titanium samples pressed with 200 MPa, also consistent with the conclusions referring to Figures 6 and 7.

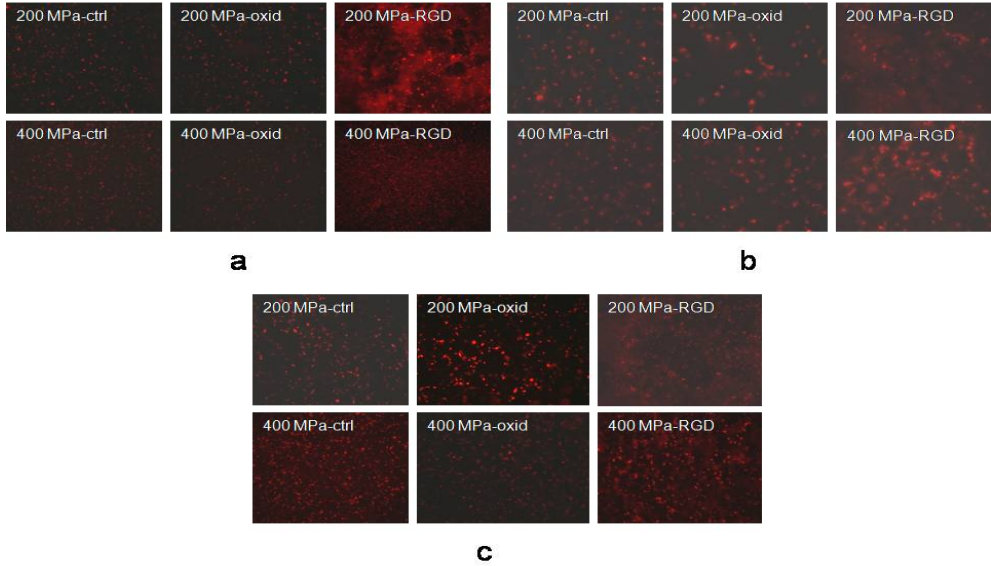


**Figure 6.** Fluorescence microscopy images (10x) of osteoblast cells stained with PKH26 dye and cultivated on different surface treatment of porous Ti substrate after 1 hour (magnification X100) (a), 4 days (magnification X200) (b) and 14 days (magnification X100) (c).

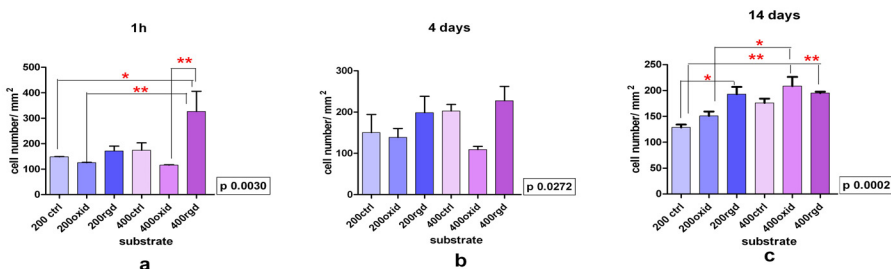


**Figure 7.** Cell counting graphs for evaluating the cell adhesion one hour after osteoblasts seeding (a) and proliferation rates of osteoblasts on different uncoated and coated titanium surfaces after 4 days (b) and 14 days (c) of cultivation.

\* indicates a significant statistical difference ( $p < 0.05$ ).

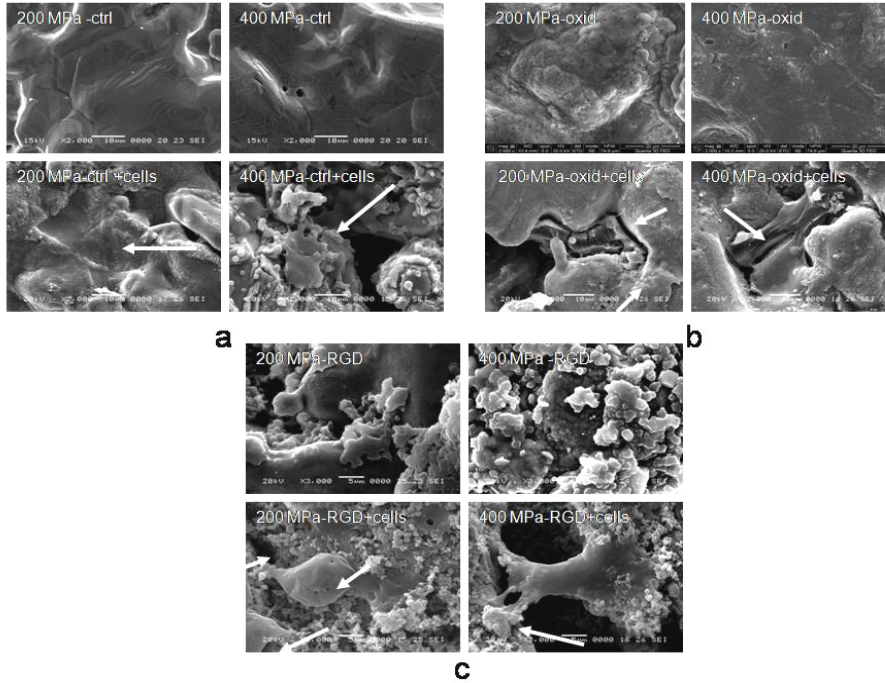


**Figure 8.** SEM micrographs of untreated titanium samples pressed with 200 MPa and 400 MPa (a), following anodizing (b) and c-RGD immobilization (c) without and with osteoblast cells after 29 days of culture. Arrows indicate adhered cells on samples surface.

## CONCLUSIONS

In this study, c-RGD peptide was successfully covalently grafted onto the surface of anodized  $\text{TiO}_2$  after coating with an intermediary layer of APTES. Furthermore, the c-RGD peptide promoted the adhesion and proliferation of osteoblast cells. The results of *in vitro* tests showed that c-RGD peptide accelerated the initial attachment of osteoblast cells, phenomenon which is not consistent for a longer time. Therefore, we believe that applying an RGD coating onto  $\text{TiO}_2$  anodically grown on porous Ti implants may contribute to the improvement of osseointegration for a design of the implant that provides also other surfaces (i.e. surfaces that were only anodized) to take over the process after the first stages after implantation (weeks time). The porosity resulted after PM processing with various compacting pressures plays also a role in the enhancement of the

biocompatibility for porous titanium. In the conditions of this work, we found that the best behaviour is unexpectedly obtained for pressing with 400 MPa before sintering, leading to a smaller porosity compared to 200 MPa pressing.

## EXPERIMENTAL SECTION

### Samples preparation

The CP Ti powder (with a purity higher than 99.5%) obtained by hydration-milling-dehydration process with powder particles size lower than 150  $\mu\text{m}$  was used to manufacture porous samples with 11.5 mm diameter. Closed die pressing was performed with 200 and 400 MPa and sintering of the specimens was carried out at 1100°C for 1h in a high vacuum furnace using a heating and cooling rate of 10°C/min and a minimum vacuum level of  $10^{-5}$  Torr was guaranteed.

Microstructural characterization of the porous titanium samples was performed on the surface by optical/ electron microscopy (Olympus GX51) and in volume by microCT (Bruker microCT analyzer).

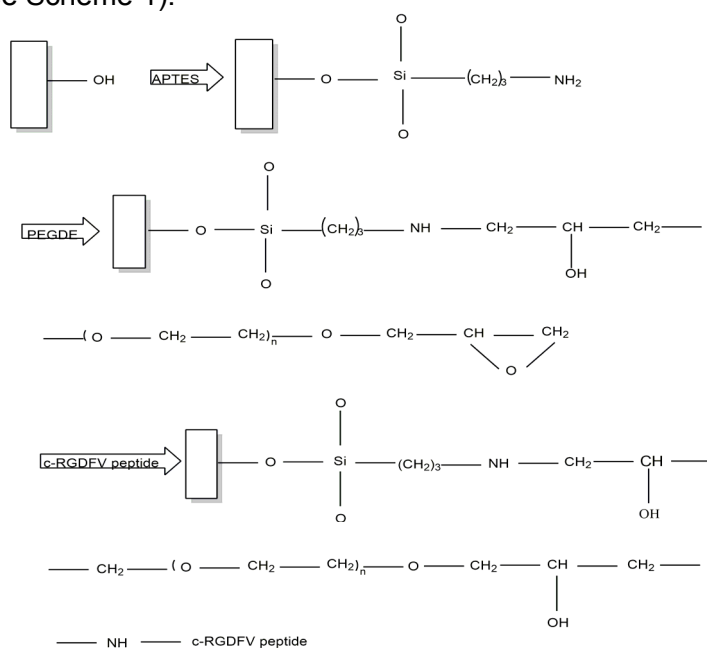
### Anodizing

Anodic oxidation was performed using a conventional three electrode cell with a porous titanium disk (samples pressed with 200 and 400 MPa) as the working electrode, a platinum electrode as the counter electrode and a saturated calomel electrode (SCE) as the reference electrode. Electrochemical measurements (chronoamperometric investigations) were conducted using a commercial potentiostat PAR 2273 at room temperature. The anodic oxidation was performed at 2V during 1hour in 0.25 M  $\text{H}_2\text{SO}_4$  solution. All solutions were prepared from reagent grade chemicals and deionized water. After the anodizing, the samples were rinsed with deionized water, dried at 60°C, and then heat treated at 700°C for 1h to crystallize the as-formed amorphous titanium oxide. The film lattice structure was examined by X-ray diffraction (Shimadzu XRD 6000).

### Silanization and c-RGD immobilization on porous titanium surfaces

Silanization of porous titanium oxidised samples was performed in 3% Aminopropyl-triethoxysilane (APTES; Sigma Aldrich) in toluene at room temperature overnight. After cleaning in toluene and ethanol, samples were cured at 110°C for 1h. Subsequently, aminosilanised Ti samples were spin coated with 3% solution of polyethyleneglycol diglycidylether (PEGDE; Sigma Aldrich) in 50 mM carbonate-buffer (pH 9), using the following parameters: 1000 rpm, 30s. The excess solution was removed by repeated rinsing with

water. After the deposition of the polyethyleneglycol diglycidylether films, the substrate was heat treated at 80°C for 2h in an oven with a heating and cooling rate of 2°C/min. RGD immobilisation was then immediately performed by spin coating with 0.5 mg/mL RGD peptide (c-RGDFV peptide, Cyclic Calbiochem) in carbonate-buffer with the same parameters presented before (see Scheme 1).



**Scheme 1.** Reaction schematic diagram for the functionalization and c-RGD peptide grafting onto anodized porous titanium: (I) APTES treatment; (II) bifunctional cross-linker (PEGDE) connection; (III) c-RGD peptide grafting.

FTIR-ATR was used to investigate the structure of APTES, PEGDE, and c-RGD films and the modification of porous titanium surface by a Perkin-Elmer FTIR model equipped with ATR accessory (PIKE MIRacle™) with diamond crystal plate.

### Cell culture

Human osteoblasts at passage eight, isolated and characterized as described by Tomuleasa et al. [26] were cultured in Dulbecco's modified Eagle's medium (DMEM) / F-12HAM (Sigma) containing 10% foetal calf serum (FCS), 2mM L-Glutamine, 1% antibiotics, 1% non-essential aminoacids (NEA) (all reagents from Sigma). Test samples were placed in 12 well plates (Nunc);  $1.2 \times 10^5$  cells were seeded in each well.

### **Cell membrane fluorescent labelling**

Fluorescent marking of osteoblasts was performed using PKH26 Red Fluorescent Cell Linker Kits (Sigma-Aldrich). This staining ensures maintenance of fluorescence of live cells for a longer period of time. After trypsinization,  $1 \times 10^6$  cells were washed twice with PBS by centrifugation at 1000 rpm, 5 min and the cell pellet was resuspended in 1ml Diluent C and 1ml of Dye Solution (4 $\mu$ l of PKH26/ml) was added, followed by gentle pipetting. The staining was stopped after 5 min by adding 2 ml of complete medium containing 10% foetal calf serum and cells were centrifuged for 10 min at 1000 rpm. Another two washing steps were performed with 10 ml of complete medium and then cells were counted, resuspended in complete medium and seeded in 12 well plates on the surface of titanium samples. The samples were formerly sterilized by immersion in 70° alcohol and exposing 3 hours to UV radiation.

### **Cell adhesion**

After 1 hour, adherent cells were visualized by fluorescence microscopy (Zeiss Axiovert D1), using filters of 546 nm and the fluorescence intensity was measured using a BioTek Synergy 2 plate reader (excitation 540 nm, emission 620 nm). We used the option of area scan in BioTek measurements that offers multiple values (13 readings) of fluorescence obtained by scanning the whole specimen surface. This is the procedure by which we obtained the final graphical representation.

### **Cell proliferation**

Cell proliferation was quantified using two methods: counting PKH26 stained cells on captured images in 3 different microscopic fields, randomly selected, and by fluorescence intensity measurements with BioTek Synergy 2 plate reader. Readings were performed at 4 days and 14 days.

### **Statistical analysis**

Statistical analysis of cell counts was performed using a GraphPad Prism 5 software, Bonferroni Multiple Comparison post-test. Statistical significance was set at  $p < 0.05$ .

### **SEM morphological analysis**

The cells were studied after 29 days of culture. Specimens were sputter coated with a gold layer using a Desk V coating device. The surface morphology of the samples with or without seeded cells was studied by scanning electron microscopy (JEOL 5600 LV).

## ACKNOWLEDGMENTS

This work was supported partially by the project STEMREG PN-II-PT-PCCA-2011-3.1-0700 and partially by the strategic grant POSDRU/159/1.5/S/137070 (2014) of the Ministry of National Education, Romania, co-financed by the European Social Fund - Investor in People, within the Sectorial Operational Programme Human Resources Development 2007-2013.

## REFERENCES

1. S. Nayak, T. Dey, D. Naskar, et al., *Biomaterials*, **2013**, 34, 2855.
2. N.A. Al-Mobarak and A.A. Al-Swayih, *Int. J. Electrochem. Sci.*, **2014**, 9, 32.
3. T. Marcu, A.M. Salantiu, I. Gligor, et al., *J. Optoelectron. Adv. Mater*, **2013**, 15, 847.
4. I. Gligor, T. Marcu, M. Todea, et al., *J. Optoelectron. Adv. Mater*, **2011**, 13, 879.
5. B. Dabrowski, W. Swieszkowski, D. Godlinski, et al., *J Biomed Mater Res B Appl Biomater* **2010**, 95, 53.
6. L.M. Reis de Vasconcellos, D. Oliveira Leite, F. Nascimento de Oliveira, et al., *Braz Oral Res*, **2010**, 24, 399.
7. D. Arya, S. Tripathi and R Bharti, *J Dent Implant*, **2012**, 2, 93.
8. A.B. Novaes Jr, S.L. Scombatti de Souza, R.R. Martins de Barros, et al., *Braz. Dent. J*, **2010**, 21, 471.
9. H.S. Kim, Y. Yang, J.T. Koh, et al., *J Biomed Mater Res Part B: Appl Biomater*, **2009**, 88B, 427–435.
10. S.Oh,K.S. Moon, S.H. Lee, *J. Nanomater*, **2013**, doi.org/10.1155/2013/965864.
11. S.Y. Park, H.S. Kim, J.H. Kim et al., *J.Tissue Eng Regener. Med.*, **2012**, 9, 194.
12. M.L. Schwarz, M. Kowarsch, S. Rose, et al., *J.Biomed Mater Res A.*, **2009**, 89, 667.
13. E.S. Gawalt, M.J. Avaltroni, M. Danahy, et al., *Langmuir*, **2003**, 19, 200.
14. G. Tan, L. Zhang, C. Ning, et al., *Thin Solid Films*, **2011**, 519, 4997.
15. E.C. Pegg, G.S. Walker, C.A. Scotchford, et al., *J. Biomed Mater Res A*, **2009**, 90, 947.
16. P. Renoud, B. Toury, S. Benayoun, et al., *PLoS ONE* 7(7): e39367.2012, **2012**, doi: 10.1371/journal.pone.0039367.
17. N. Aissaoui, L. Bergaoui, J. Landoulsi, et al., *Langmuir*, **2012**, 28, 656.
18. G. Forget, L. Latxague, V. Héroguez, et al. In: *Conf. Proc. IEEE Eng Med Biol Soc.* **2007**, 5107.
19. P.W. Kämmerer, M. Heller, J. Brieger, et al., *Eur Cell Mater* **2011**, 21, 364-372.
20. M. Dettin, T. Herath, R. Gambaretto, et al., *J.Biomed Mater Res A.*, **2009**, 1, 463.
21. H. Huang, Y. Zhao, Z. Liu, et al., *J Oral Implantol.* **2003**, 29, 73.
22. J. Kim, P. Seidler, L.S. Wan, et al., *J. Colloid Interface Sci.*, **2009**, 329, 114-119.
23. J.P. Matinlinna, S. Areva, L.V.J. Lassila, et al., *Surf. Interface Anal.*, **2004**, 36, 1314-1322.
24. T.T. Nguyen, M. Raupach and L.J. Janik, *Clays Clay Miner*, **1987**, 35, 60-67.
25. J. Zhu, C. Tang, K. Kottke-Marchant, et al., *Bioconjug Chem.*, **2009**, 20, 333-339.
26. C.I. Tomuleasa, V. Foris, O. Soritau, et al., *Rom. J. Morphol. Embryol.*, **2009**, 50, 349-355.